

Localization of Elliptic Multiscale Problems

Axel Målqvist ^{*} [†] Daniel Peterseim [‡] [§]

March 22, 2012

Abstract

This paper constructs a local generalized finite element basis for elliptic problems with heterogeneous and highly varying diffusion coefficient. The basis functions are solutions to local problems on vertex patches. The error of the corresponding generalized finite element method decays exponentially with respect to the number of layers of elements in the patches. Hence, on a uniform mesh of size H , patches of diameter $H \log(1/H)$ are sufficient to preserve a linear rate of convergence in H without pre-asymptotic effects. The analysis does not rely on regularity of the solution or scale separation in the coefficient. This result motivates new and justifies old classes of variational multiscale methods.

Keywords finite element method, a priori error estimate, convergence, multiscale method

AMS subject classifications 65N12, 65N30

1 Introduction

This paper considers the numerical solution of second order elliptic problems with strongly heterogeneous and highly varying (non-periodic) diffusion coefficient.

^{*}Department of Information Technology, Uppsala University, Box 337, SE-751 05 Uppsala, Sweden

[†]The first author is supported by The Göran Gustafsson Foundation and The Swedish Research Council.

[‡]Institut für Mathematik, Humboldt-Universität zu Berlin, Unter den Linden 6, D-10099 Berlin, Germany

[§]The second author is supported by the DFG Research Center Matheon Berlin through project C33.

cient. The heterogeneities and oscillations of the coefficient may appear on several non-separated scales. It is well known that classical polynomial based finite element methods perform arbitrarily badly for such problems, see e.g. [4]. To overcome this lack of performance, many methods that are based on general (non-polynomial) ansatz functions have been developed. Early works [3, 1], that essentially apply to one dimensional problems, have been generalized to the multi-dimensional case in several ways during the last fifteen years, see e.g. [13, 12, 7]. In these methods the problem is split into coarse and (possibly several) fine scales. The fine scale effect on the coarse scale is either computed numerically or modeled analytically. The resulting modified coarse problem can then be solved numerically and its solution contains crucial information from the fine scales. Although many of these approaches show promising results in practice, their convergence analysis usually assumes certain periodicity and scale separation.

For problems with general L^∞ coefficient, the paper [2] gives error bounds for a generalized finite element method that involves the solutions of local eigenvalue problems. The construction in [6, 21] depends only on the solution of the original problem on certain subdomains. However, the size of these subdomains strongly depends on the mesh size. This dependence is suboptimal with respect to the theoretical statement given in [11], that is, for any shape regular mesh of size H there exist $O((\log(1/H))^{d+1})$ local (non-polynomial) basis functions per nodal point such that the error of the corresponding Galerkin solution u_H satisfies the estimate $\|u - u_H\|_{H^1(\Omega)} \leq C_f H$ with a constant C_f that depends on f and the global bounds of the diffusion coefficient but not on its variations. The derivation in [11] is not constructive in the sense that it involves the solution of the (global) original problem with specific right hand sides.

In this paper, we show that such a (quasi-)optimal basis can indeed be constructed by solving only local problems on element patches. We use a modified nodal basis similar to the one presented in [15] and prove that these basis functions decay exponentially away from the node they are associated with. This exponential decay justifies an approximation of localized patches.

The precise setting of the paper is as follows. Let $\Omega \subset \mathbb{R}^d$ be a bounded Lipschitz domain with polygonal boundary and let the diffusion matrix $A \in L^\infty(\Omega, \mathbb{R}_{\text{sym}}^{d \times d})$ be uniformly elliptic:

$$\begin{aligned}
0 < \alpha(A, \Omega) &:= \operatorname{ess\,inf}_{x \in \Omega} \inf_{v \in \mathbb{R}^d \setminus \{0\}} \frac{\langle A(x)v, v \rangle}{\langle v, v \rangle}, \\
\infty > \beta(A, \Omega) &:= \operatorname{ess\,sup}_{x \in \Omega} \sup_{v \in \mathbb{R}^d \setminus \{0\}} \frac{\langle A(x)v, v \rangle}{\langle v, v \rangle}.
\end{aligned} \tag{1}$$

Given $f \in L^2(\Omega)$, we seek $u \in V := H_0^1(\Omega)$ such that

$$a(u, v) := \int_{\Omega} \langle A \nabla u, \nabla v \rangle dx = \int_{\Omega} f v dx =: F(v) \quad \text{for all } v \in V. \quad (2)$$

The bilinear form a is symmetric, coercive, bounded, and hence, (2) has a unique solution.

The main result of this paper (cf. Theorem 8) shows that the error $u - u_{H,k}^{\text{ms}}$ of the generalized finite element method, which is based on our new (local) basis functions mentioned above, is bounded as follows

$$\|A^{1/2} \nabla(u - u_{H,k}^{\text{ms}})\| \leq C_f H;$$

H being the mesh size of the underlying coarse finite element mesh and $k \approx \log(1/H)$ referring to the number of element layers that form the support of the localized basis functions. This result establishes the first error bound for a numerical upscaling procedure beyond periodicity and scale separation. Moreover, this result is stable with respect to perturbations arising from the discretization of the local problems. These results give a theoretical foundation for numerous previous experiments where the exponential decay of a similar modified basis has been noticed, see e.g. [18].

The outline of the paper is as follows. In Section 2, we derive a set of local basis functions and define the corresponding multiscale finite element method. The error analysis is done in Section 3. Section 4 is devoted to the discretization of the local problems. Section 5 presents numerical experiments, and Section 6 discusses the application of this theory to state-of-the-art multiscale methods.

2 Local Basis

In this section, we design a set of local basis functions for the multiscale problem under consideration. The construction is based on a regular (in the sense of [9]) finite element mesh \mathcal{T}_H of Ω into closed triangles ($d = 2$) or tetrahedra ($d = 3$). Subsection 2.1 recalls the classical nodal basis with respect to \mathcal{T}_H and demonstrates its lack of approximation properties. Subsection 2.3 defines a modified (coefficient dependent) nodal basis and analyzes its approximation properties. This basis is then localized in Subsection 2.4.

2.1 Classical Nodal Basis

Let $H : \bar{\Omega} \rightarrow \mathbb{R}_{>0}$ denote the \mathcal{T}_H -piecewise constant mesh size function with $H|_T = \text{diam}(T) =: H_T$ for all $T \in \mathcal{T}_H$. The mesh size may vary in space. In

practical applications, the mesh \mathcal{T}_H (resp. its size H) shall be determined by the accuracy which is desired or the computational capacity that is available but *not* by the scales of the coefficient.

The classical (conforming) P_1 finite element space is given by

$$S_H := \{v \in C^0(\bar{\Omega}) \mid \forall T \in \mathcal{T}_H, v|_T \text{ is a polynomial of total degree } \leq 1\}. \quad (3.a)$$

Let $V_H := S_H \cap V$ denote the space of finite element functions that match the homogeneous Dirichlet boundary condition. Let \mathcal{N} denote the set of interior vertices of \mathcal{T}_H . For every vertex $x \in \mathcal{N}$, let $\lambda_x \in S_H$ denote the corresponding nodal basis function (tent function), i.e.,

$$\lambda_x(x) = 1 \quad \text{and} \quad \lambda_x(y) = 0 \quad \text{for all } y \neq x \in \mathcal{N}.$$

These nodal basis functions form a basis of V_H . The availability of such a local basis is a key property of any finite element method and ensures that the resulting linear system is sparse.

The (unique) Galerkin approximation $u_H \in V_H$ satisfies

$$a(u_H, v) = F(v) \quad \text{for all } v \in V_H. \quad (3.b)$$

The above method (3) is optimal with respect to the energy norm $\|\cdot\| := \|\cdot\|_{\Omega} := \|A^{1/2} \nabla \cdot\|_{L^2(\Omega)}$ on V which is induced by a ,

$$\|u - u_H\| = \min_{v_H \in V_H} \|u - v_H\|. \quad (4)$$

Assuming that the solution u is smooth, the combination of (4) and standard interpolation error estimates yields the standard a priori error estimate

$$\|u - u_H\| \leq C \|H\|_{L^\infty(\Omega)} \|\nabla^2 u\|_{L^2(\Omega)}.$$

This estimate states linear convergence of the classical finite element method (3) as the maximal mesh width tends to zero. However, the regularity assumption is not realistic for the problem class under consideration. Moreover, even if the coefficient is smooth, it may oscillate rapidly, say at frequency ε^{-1} for some small parameter ε . In this case, the asymptotic result is useless because $\nabla^2 u$ may oscillate at the same scale, a fact that is hidden in the constant $\|\nabla^2 u\|_{L^2(\Omega)} \approx \varepsilon^{-1}$. Unless $H \lesssim \varepsilon$, the above finite element space is unable to capture the behavior of the solution neither on the microscopic nor on the macroscopic level. In what follows, we present a modification of this method that resolves this issue.

2.2 Quasi Interpolation

The key tool in our construction will be some bounded linear surjective (quasi-) interpolation operator $\mathfrak{I}_H : V \rightarrow V_H$. The choice of this operator is not unique and a different choice leads to a different multiscale method. We have in mind the following modification of Clément's interpolation [10] which is presented and analyzed in [8, Section 6]. Given $v \in V$, $\mathfrak{I}_H v := \sum_{x \in \mathcal{N}} (\mathfrak{I}_H v)(x) \lambda_x$ defines a (weighted) Clément interpolant with nodal values

$$(\mathfrak{I}_H v)(x) := \left(\int_{\Omega} v \lambda_x \, dx \right) / \left(\int_{\Omega} \lambda_x \, dx \right) \quad (5)$$

for $x \in \mathcal{N}$. The nodal values are weighted averages of the function over nodal patches $\omega_x := \text{supp } \lambda_x$. Since the summation is taken only with respect to interior vertices \mathcal{N} , this operator matches homogeneous Dirichlet boundary conditions.

Recall the (local) approximation and stability properties of the interpolation operator \mathfrak{I}_H [8, Section 6]: There exists a generic constant $C_{\mathfrak{I}_H}$ such that for all $v \in V$ and for all $T \in \mathcal{T}_H$ it holds

$$H_T^{-1} \|v - \mathfrak{I}_H v\|_{L^2(T)} + \|\nabla(v - \mathfrak{I}_H v)\|_{L^2(T)} \leq C_{\mathfrak{I}_H} \|\nabla v\|_{L^2(\omega_T)} \quad (6.a)$$

with $\omega_T := \cup\{K \in \mathcal{T}_H \mid T \cap K \neq \emptyset\}$. The constant $C_{\mathfrak{I}_H}$ depends on the shape regularity parameter ρ of the finite element mesh \mathcal{T}_H (see (13) below) but not on $\text{diam } T$.

The above interpolation operator is not a projection, i.e., $v_H \in V_H$ does not equal its interpolation $\mathfrak{I}_H v_H$ in general. However, the particular choice gives rise to the following lemma.

Lemma 1 *There exists a generic constant $C'_{\mathfrak{I}_H}$ which only depends on ρ but not on the local mesh size H , such that for all $v_H \in V_H$ there exists $v \in V$ such that*

$$\mathfrak{I}_H(v) = v_H \quad \text{and} \quad \|v\| \leq C'_{\mathfrak{I}_H} \|v_H\| \quad \text{and} \quad \text{supp } v \subset \text{supp } v_H. \quad (6.b)$$

Proof. For every nodal basis function λ_x , $x \in \mathcal{N}$, there is a $\beta_x \in H_0^1(\omega_x)$ such that $\mathfrak{I}_H(\beta_x) = \lambda_x$ and $\|\beta_x\| \leq C''_{\mathfrak{I}_H} \|\lambda_x\|$ with some constant $C''_{\mathfrak{I}_H}$ that does not depend on x and H . Note that β_x may be chosen from the finite element space that is related to some uniform refinement of \mathcal{T}_H .

Given $v_H = \sum_{x \in \mathcal{N}} v_H(x) \lambda_x \in V_H$, $v := v_H + \sum_{x \in \mathcal{N}} (v_H(x) - (\mathfrak{I}_H v_H)(x)) \beta_x \in V$ has the desired properties. The interpolation and support properties are obvious.

The stability follows from

$$\begin{aligned}
\|v\|^2 &\leq C \left(\|v_H\|^2 + \sum_{x \in \mathcal{N}} |v_H(x) - (\mathfrak{I}_H v_H)(x)|^2 \|\beta_x\|^2 \right) \\
&\leq C \left(\|v_H\|^2 + C_{\mathfrak{I}_H}''^2 \sum_{x \in \mathcal{N}} |v_H(x) - (\mathfrak{I}_H v_H)(x)|^2 \|\lambda_x\|^2 \right) \\
&\leq C \left(\|v_H\|^2 + C' C_{\mathfrak{I}_H}''^2 \sum_{T \in \mathcal{T}_H} \|v_H - \mathfrak{I}_H v_H\|_{L^2(T)}^2 H_T^{-2} \right) \\
&\leq C \left(\|v_H\|^2 + C' C_{\mathfrak{I}_H}^2 C_{\mathfrak{I}_H}''^2 \sum_{T \in \mathcal{T}_H} \|\nabla v_H\|_{L^2(\omega_T)}^2 \right) \\
&\leq C_{\mathfrak{I}_H}'^2 \|v_H\|^2,
\end{aligned}$$

where we have used $\|\lambda_x\|^2 \approx |\text{supp } \lambda_x|^{(d-2)}$, the inverse inequality $\|v_H - \mathfrak{I}_H v_H\|_{L^\infty(T)}^2 \lesssim H_T^{-d} \|v_H - \mathfrak{I}_H v_H\|_{L^2(T)}^2$, and (6.a). ■

In what follows the interpolation operator (5) may be replaced by any linear bounded surjective operator that satisfies (6.a)–(6.b). Hereby, (6.b) may be relaxed in the sense that $\text{supp } v$ is not necessarily a subset of $\text{supp } v_H$ but that $\text{supp } v \setminus \text{supp } v_H$ covers at most a fixed (small) number of element layers about $\text{supp } v_H$.

2.3 Multiscale Splitting and Modified Nodal Basis

Let $\mathfrak{I}_H : V \rightarrow V_H$ be a quasi interpolation operator according to the previous subsection. Then the kernel of \mathfrak{I}_H

$$V^f := \{v \in V \mid \mathfrak{I}_H v = 0\}$$

represents the microscopic features of V , i.e., all features that are not captured by V_H . Given $v \in V_H$, define $\mathfrak{F}v \in V^f$ by

$$a(\mathfrak{F}v, w) = a(v, w) \quad \text{for all } w \in V^f.$$

The finescale projection operator $\mathfrak{F} : V_H \rightarrow V^f$ leads to an orthogonal splitting with respect to the scalar product a

$$V = V_H^{\text{ms}} \oplus V^f \quad \text{where} \quad V_H^{\text{ms}} := (V_H - \mathfrak{F}V_H).$$

Hence, any function $u \in V$ can be decomposed into $u_H^{\text{ms}} \in V_H^{\text{ms}}$ and $u^f \in V^f$, $u = u_H^{\text{ms}} + u^f$, with $a(u_H^{\text{ms}}, u^f) = 0$. Since $\dim V_H^{\text{ms}} = \dim V_H$, the space V_H^{ms} can

be regarded as a modified coarse space. The superscript “ms” abbreviates “multiscale” and indicates that V_H^{ms} , in addition, contains fine scale information. The corresponding Galerkin approximation $u_H^{\text{ms}} \in V_H^{\text{ms}}$ satisfies

$$a(u_H^{\text{ms}}, v) = F(v) \quad \text{for all } v \in V_H^{\text{ms}}. \quad (7)$$

The error $(u - u_H^{\text{ms}})$ of the above method (7) is analyzed in Section 3.1.

Finally, we shall introduce a basis of V_H^{ms} . The image of the nodal basis function λ_x under the fine scale projection \mathfrak{F} is denoted by $\phi_x = \mathfrak{F}\lambda_x \in V^f$, i.e., ϕ_x satisfies the corrector problem

$$a(\phi_x, w) = a(\lambda_x, w) \quad \text{for all } w \in V^f. \quad (8)$$

A basis of V_H^{ms} is then given by the modified nodal basis

$$\{\lambda_x - \phi_x \mid x \in \mathcal{N}\}. \quad (9)$$

In general, the corrections ϕ_x of nodal basis functions λ_x , $x \in \mathcal{N}$, have global support, a fact which limits the practical use of the modified basis (9) and the corresponding method (7).

2.4 Localization

In Section 3.2, we will show that the correction ϕ_x decays exponentially fast away from x . Hence, simple truncation of the corrector problems to local patches of coarse elements yields localized basis functions with good approximation properties.

Let $k \in \mathbb{N}$. Define nodal patches of k -th order ω_x^k about $x \in \mathcal{N}$ by

$$\begin{aligned} \omega_{x,1} &:= \text{supp } \lambda_x = \text{int}(\cup \{T \in \mathcal{T}_H \mid x \in T\}), \\ \omega_{x,k} &:= \text{int}(\cup \{T \in \mathcal{T}_H \mid T \cap \bar{\omega}_{x,k-1} \neq \emptyset\}), \quad k = 2, 3, 4, \dots \end{aligned} \quad (10)$$

Define localized finescale spaces $V^f(\omega_{x,k}) := \{v \in V^f \mid v|_{\Omega \setminus \omega_{x,k}} = 0\}$, $x \in \mathcal{N}$, by intersecting V^f with those functions that vanish outside the patch $\omega_{x,k}$. The solutions $\phi_{x,k} \in V^f(\omega_{x,k})$ of

$$a(\phi_{x,k}, w) = a(\lambda_x, w) \quad \text{for all } w \in V^f(\omega_{x,k}), \quad (11)$$

are approximations of ϕ_x from (8) with local support.

We define localized multiscale finite element spaces

$$V_{H,k}^{\text{ms}} = \text{span}\{\lambda_x - \phi_{x,k} \mid x \in \mathcal{N}\} \subset V. \quad (12.a)$$

The corresponding multiscale approximation of (2) reads: find $u_{H,k}^{\text{ms}} \in V_{H,k}^{\text{ms}}$ such that

$$a(u_{H,k}^{\text{ms}}, v) = F(v) \quad \text{for all } v \in V_{H,k}^{\text{ms}}. \quad (12.b)$$

Note that $\dim V_{H,k}^{\text{ms}} = |\mathcal{N}| = \dim V_H$, i.e., the number of degrees of freedom of the proposed method (12) is the same as for the classical method (3). The basis functions of the multiscale method have local support. The overlap is proportional to the parameter k . The error analysis of Section 3.2 suggests to choose $k \approx \log \frac{1}{H}$.

Remark 2 *The localized modified basis functions could be localized further to vertex patches ω_x , $x \in \mathcal{N}$, by simply multiplying them with the classical nodal basis functions; for any $x \in \mathcal{N}$ and any $y \in \mathcal{N} \cap \omega_{x,k}$, define $\phi_x^y := \lambda_y \phi_{x,k}$. The generalized finite element space which is spanned by those $O((\log(1/H))^d)$ local basis functions per vertex has similar approximation properties as $V_{H,k}^{\text{ms}}$ (see [5]).*

3 Error Analysis

This section analyzes the proposed multiscale method in two steps. First, Subsection 3.1 presents an error bound for the idealized method (7). Then, Subsection 3.2 bounds the error of truncation to local patches and proves the main result, that is, an error bound for the multiscale method (12).

As usual, the error analysis depends on the constant $\rho > 0$ which represents shape regularity of the finite element mesh \mathcal{T}_H :

$$\rho := \max_{T \in \mathcal{T}_H} \rho_T \quad \text{with} \quad \rho_T := \frac{\text{diam } B_T}{\text{diam } T} \quad \text{for } T \in \mathcal{T}_H, \quad (13)$$

where B_T denotes the largest ball contained in T .

3.1 Discretization Error

Lemma 3 *Let $u \in V$ solve (2) and $u_H^{\text{ms}} \in V_H^{\text{ms}}$ solve (7). Then it holds*

$$\|u - u_H^{\text{ms}}\| \leq C_{\text{ol}}^{1/2} C_{\mathfrak{S}_H} \alpha^{-1} \|Hf\|_{L^2(\Omega)}$$

with constants C_{ol} and $C_{\mathfrak{S}_H}$ that only depend on ρ .

Proof. Recall the (local) approximation and stability properties (6.a) of the interpolation operator \mathfrak{S}_H . Due to the splitting from Section 2.3, it holds $u - u_H^{\text{ms}} = u^f$.

Since $\mathfrak{I}_H u^f = 0$, the application of (6.a) and Young's inequality yield

$$\begin{aligned} \|\|u^f\|\|^2 &= F(u^f) \leq \sum_{T \in \mathcal{T}_H} \|f\|_{L^2(T)} \|u^f - \mathfrak{I}_H u^f\|_{L^2(T)} \\ &\leq \frac{C_{\mathfrak{I}_H}^2}{2\epsilon\alpha^2} \|Hf\|_{L^2(\Omega)}^2 + \frac{\epsilon}{2} \sum_{T \in \mathcal{T}_H} \|A^{1/2} \nabla u^f\|_{L^2(\omega_T)}^2 \end{aligned}$$

for any $\epsilon > 0$. Note that there exists a constant $C_{\text{ol}} > 0$ that only depends on ρ such that the number of elements covered by ω_T is uniformly bounded (w.r.t. T) by C_{ol} . The choice $\epsilon = C_{\text{ol}}^{-1}$ concludes the proof. ■

Remark 4 Substituting \mathfrak{I}_H by the modified Clément interpolation operator presented in [10] allows one to replace the term $\|Hf\|_{L^2(\Omega)}$ in Lemma (3) by data oscillations $(\sum_{x \in \mathcal{N}} \|H(f - f_x)\|_{L^2(\omega_x)}^2)^{1/2}$ with some weighted averages f_x of f on ω_x , $x \in \mathcal{N}$; we refer to [10, Section 2] for details.

3.2 Error of Localized Multiscale FEM

First, we estimate the error due to truncation to local patches. We will frequently make use of cut-off functions on element patches.

Definition 5 For $x \in \mathcal{N}$ and $d < D \in \mathbb{N}$, let $\eta_x^{d,D} : \Omega \rightarrow [0, 1]$ be a continuous and weakly differentiable function such that

$$(\eta_x^{d,D})|_{\omega_{x,d}} = 0, \quad (14.a)$$

$$(\eta_x^{d,D})|_{\Omega \setminus \omega_{x,D}} = 1, \text{ and} \quad (14.b)$$

$$\forall T \in \mathcal{T}_H, \|\nabla \eta_x\|_{L^\infty(T)} \leq C_{\text{co}}(D-d)^{-1} H_T^{-1} \quad (14.c)$$

with some constant C_{co} that only depends on ρ . For example, one may choose $\eta_x^{d,D} \in S_H$ with nodal values

$$\begin{aligned} \eta_x^{d,D}(x) &= 0 \quad \text{for all } x \in \mathcal{N} \cap \omega_d, \\ \eta_x^{d,D}(x) &= 1 \quad \text{for all } x \in \mathcal{N} \cap (\Omega \setminus \omega_{x,D}), \text{ and} \\ \eta_x^{d,D}(x) &= m(D-d)^{-1} \quad \text{for all } x \in \mathcal{N} \cap \partial\omega_{x,d+m}, \quad m = 0, 1, 2, \dots, D-d. \end{aligned} \quad (15)$$

Lemma 6 For all $x \in \mathcal{N}$, $k, \ell \geq 2 \in \mathbb{N}$ the estimate

$$\|\|\phi_x - \phi_{x,\ell k}\|\| \leq C_2 \left(\frac{C_1}{\ell}\right)^{\frac{k-2}{2}} \|\|\phi_x\|\|_{\omega_{x,\ell}}$$

holds with constants C_1, C_2 that only depend on ρ but not on x, k, ℓ , or H .

Proof. Let $x \in \mathcal{N}$ and $\ell, k \geq 2 \in \mathbb{N}$. Observe that

$$\|\phi_x - \phi_{x,\ell k}\|^2 \leq \|\phi_x - v\|^2 = \|\phi_x - v\|_{\omega_{x,\ell k}}^2 + \|\phi_x\|_{\Omega \setminus \omega_{x,\ell k}}^2, \quad (16)$$

holds for all $v \in V^f(\omega_{x,\ell k})$ using Galerkin orthogonality.

Let $\zeta_x := 1 - \eta_x^{\ell(k-1)+1, \ell k-1}$ with a cutoff function $\eta_x^{\ell(k-1)+1, \ell k-1}$ as in Definition 5. According to (6.b), there exists $b_x \in V$ such that $\mathfrak{I}_H(b_x) = \mathfrak{I}_H(\zeta_x \phi_x)$, $\|b_x\| \lesssim \|\mathfrak{I}_H(\zeta_x \phi_x)\|$, and $\text{supp}(b_x) \subset \omega_{x,\ell k}$. Hence, $v := \zeta_x \phi_x - b_x \in V^f(\omega_{x,\ell k})$ and

$$\begin{aligned} \|\phi_x - v\|_{\omega_{x,\ell k}} &\leq \|\phi_x - \zeta_x \phi_x\|_{\omega_{x,\ell k} \setminus \omega_{x,\ell(k-1)+1}} + \|b_x\|_{\omega_{x,\ell k} \setminus \omega_{x,\ell(k-1)}} \\ &\leq C'_{\mathfrak{I}_H} C_{\mathfrak{I}_H} \left(\|\phi_x\|_{\omega_{x,\ell k} \setminus \omega_{x,\ell(k-1)+1}} + \|\zeta_x \phi_x\|_{\omega_{x,\ell k} \setminus \omega_{x,\ell(k-1)}} \right). \end{aligned}$$

Since $\mathfrak{I}_H \phi_x = 0$, the upper bound of the interpolation error (6.a) and (14.c) yield

$$\begin{aligned} \|\zeta_x \phi_x\|_{\omega_{x,\ell k} \setminus \omega_{x,\ell(k-1)}}^2 &\leq \sum_{T \in \mathcal{T}_H: T \subset \bar{\omega}_{x,\ell k} \setminus \omega_{x,\ell(k-1)+1}} \|\nabla \zeta_k\|_{L^\infty(T)}^2 \|A^{1/2} \phi_x\|_{L^2(T)}^2 + \|\zeta_k\|_{L^\infty(T)}^2 \|\phi_x\|_{L^2(T)}^2 \\ &\leq C''_2 \|\phi_x\|_{\omega_{x,\ell k} \setminus \omega_{x,\ell(k-1)+1}}^2 \end{aligned}$$

with $C''_2 := 1 + C_{\text{oi}} C_{\text{co}}^2 C_{\mathfrak{I}_H}^2 C_A$ and $C_A := \max_{T \in \mathcal{T}_H} \frac{\beta(A,T)}{\alpha(A,T)}$. This leads to

$$\|\phi_x - v\|_{\omega_{x,\ell k}} \leq C'_2 \|\phi_x\|_{\omega_{x,\ell k} \setminus \omega_{x,\ell(k-1)\ell}}. \quad (17)$$

The combination of (16), with $v = \zeta_x \phi_x - b_x$, and (17) yields

$$\|\phi_x - \phi_{x,\ell k}\| \leq C_2 \|\phi_x\|_{\Omega \setminus \omega_{x,\ell(k-1)}}. \quad (18)$$

Further estimation of the right hand side in (18) is possible using cutoff functions $\eta_j := \eta_x^{\ell(j-1)+1, \ell j}$ (cf. Definition 5), $j = 2, 3, \dots, k-1$. Observe that

$$\begin{aligned} \|A^{1/2} \nabla \phi_x\|_{L^2(\Omega \setminus \omega_{x,\ell(k-1)})}^2 &\leq \|A^{1/2} \eta_{k-1} \nabla \phi_x\|_{L^2(\Omega)}^2 \\ &= \int_{\Omega} \langle A \nabla \phi_x, \nabla(\eta_{k-1}^2 \phi_x) \rangle dx - 2 \int_{\Omega} \eta_{k-1} \phi_x \langle A \nabla \phi_x, \nabla \eta_{k-1} \rangle dx. \end{aligned} \quad (19)$$

Let, according to Lemma 1, $b_{x,(k-1)}$ be chosen such that $\mathfrak{I}_H b_{x,(k-1)} = \mathfrak{I}_H(\eta_{k-1}^2 \phi_x)$. Then $\eta_{k-1}^2 \phi_x - b_{x,(k-1)} \in V^f$. Since $|\text{supp}(\nabla \lambda_x) \cap \text{supp}(\eta_{k-1})| = 0$ and $\text{supp}(\nabla \eta_{k-1}) = \omega_{x,(k-1)\ell} \setminus \omega_{x,(k-2)\ell+1}$, the first term on the right-hand side of (19) can be rewritten as

$$\begin{aligned} &\int_{\Omega} \langle A \nabla \phi_x, \nabla(\eta_{k-1}^2 \phi_x) \rangle dx \\ &= \int_{\Omega} \langle A \nabla \phi_x, \nabla(\eta_{k-1}^2 \phi_x - b_{x,(k-1)}) \rangle dx + \int_{\Omega} \langle A \nabla \phi_x, \nabla b_{x,(k-1)} \rangle dx \\ &= \int_{\Omega} \langle A \nabla \phi_x, \nabla b_{x,(k-1)} \rangle dx \\ &\leq C'_{\mathfrak{I}_H} C_{\mathfrak{I}_H} \|\phi_x\|_{\omega_{x,(k-1)\ell} \setminus \omega_{x,(k-2)\ell+1}} \|\mathfrak{I}_H(\eta_{k-1}^2 \phi_x)\|_{\omega_{x,(k-1)\ell} \setminus \omega_{x,(k-2)\ell+1}}. \end{aligned} \quad (20)$$

With $\overline{\eta_T^2} := |T|^{-1} \int_T \eta_{k-1}^2 \, dx$ we have

$$\begin{aligned} \left\| \mathfrak{S}_H(\eta_{k-1}^2 \phi_x) \right\|_T &= \left\| \mathfrak{S}_H((\eta_{k-1}^2 - \overline{\eta_T^2}) \phi_x) \right\|_T \leq C_{\mathfrak{S}_H} \left\| (\eta_{k-1}^2 - \overline{\eta_T^2}) \phi_x \right\|_T \\ &\leq C_{\mathfrak{S}_H} \left(\|(\eta_{k-1}^2 - \overline{\eta_T^2})\|_{L^\infty(T)} \|\phi_x\|_T + \|\nabla(\eta_{k-1}^2)\|_{L^\infty(T)} \sqrt{\beta_T} \|\phi_x\|_{L^2(T)} \right) \\ &\leq 2C_{\mathfrak{S}_H} \|\nabla(\eta_{k-1})\|_{L^\infty(T)} \left(\text{diam}(T) \|\phi_x\|_T + \sqrt{\beta_T} \|\phi_x - \mathfrak{S}_H(\phi_x)\|_{L^2(T)} \right). \end{aligned}$$

Thus the property (14.c) of the cutoff function and the upper bound of the interpolation error (6.a) yield

$$\left\| \mathfrak{S}_H(\eta_{k-1}^2 \phi_x) \right\|_{\omega_{x,(k-1)\ell} \setminus \omega_{x,(k-2)\ell+1}} \leq C'_1 \ell^{-1} \|A^{1/2} \nabla \phi_x\|_{L^2(\Omega \setminus \omega_{x,(k-2)\ell})}, \quad (21)$$

where C'_1 only depends on $C_{\mathfrak{S}_H}$, C_{co} , C_{ol} , and C_A . The same arguments allow one to bound the second term on the right-hand side in (19)

$$\begin{aligned} &2 \int_{\Omega} \eta_{k-1} \phi_x \langle A \nabla \phi_x, \nabla \eta_{k-1} \rangle \, dx \\ &\leq 2 \sum_{T \in \mathcal{T}_H: T \subset \overline{\omega_{x,(k-1)\ell}} \setminus \omega_{x,(k-2)\ell+1}} \|\nabla \eta_{k-1}\|_{L^\infty(T)} \|A^{1/2} \nabla \phi_x\|_{L^2(T)} \|A^{1/2} \phi_x\|_{L^2(T)} \\ &\leq C''_1 \ell^{-1} \|A^{1/2} \nabla \phi_x\|_{L^2(\Omega \setminus \omega_{x,(k-2)\ell})}^2, \end{aligned} \quad (22)$$

where C''_1 only depends on $C_{\mathfrak{S}_H}$, C_{co} , and C_A . The combination of (19)–(22) yields

$$\|A^{1/2} \nabla \phi_x\|_{L^2(\Omega \setminus \omega_{x,(k-1)\ell})}^2 \leq C_1 \ell^{-1} \|A^{1/2} \nabla \phi_x\|_{L^2(\Omega \setminus \omega_{x,(k-2)\ell})}^2, \quad (23)$$

where $C_1 := C'_1 + C''_1$. For $j = k-2, \dots, 2$, a similar argument (with η_{k-1} replaced by η_j) yields

$$\|A^{1/2} \nabla \phi_x\|_{L^2(\Omega \setminus \omega_{x,j\ell})}^2 \leq C_1 \ell^{-1} \|A^{1/2} \nabla \phi_x\|_{L^2(\Omega \setminus \omega_{x,(j-1)\ell})}^2. \quad (24)$$

Starting from (23), the successive application of (24) for $j = k-2, k-3, \dots, 2$ proves

$$\|A^{1/2} \nabla \phi_x\|_{L^2(\Omega \setminus \omega_{x,(k-1)\ell})}^2 \leq (C_1 \ell^{-1})^{k-2} \|A^{1/2} \nabla \phi_x\|_{L^2(\omega_{x,\ell})}^2. \quad (25)$$

Combining (18) and (25), we finally obtain the assertion. ■

Lemma 7 *There is a constant C_3 that depends only on ρ and β/α , but not on $|\mathcal{N}|$, k , or ℓ such that*

$$\left\| \sum_{x \in \mathcal{N}} v(x) (\phi_x - \phi_{x,\ell k}) \right\|^2 \leq C_3 (\ell k)^d \sum_{x \in \mathcal{N}} v^2(x) \|\phi_x - \phi_{x,\ell k}\|^2.$$

Proof. For $x \in \mathcal{N}$, let $\zeta_x = 1 - \eta_x^{\ell k+1, \ell k+2}$ (cf. Definition 5). By Lemma 1 there exists a function $b_x \in V$ such that for any $w \in V^f$ it holds $\mathfrak{S}_H b_x = \mathfrak{S}_H((1 - \zeta_x)w)$, $\text{supp}(b_x) \subset \text{supp}(\mathfrak{S}_H((1 - \zeta_x)w)) \subset \omega_{x, \ell k+3} \setminus \omega_{x, \ell k}$, and $\|b_x\|_{\omega_{x, \ell k+3} \setminus \omega_{x, \ell k}} \leq C'_{\mathfrak{S}_H} \|\mathfrak{S}_H((1 - \zeta_x)w)\|_{\omega_{x, \ell k+3} \setminus \omega_{x, \ell k}}$. We note that $w - \zeta_x w - b_x \in V^f$ with support outside $\omega_{x, \ell k}$, i.e., $a(\phi_x, w - \zeta_x w - b_x) = a(\lambda_x, w - \zeta_x w - b_x) = 0$ and $a(\phi_{x, \ell k}, w - \zeta_x w - b_x) = 0$. With $w = \sum_{x \in \mathcal{N}} v(x)(\phi_x - \phi_{x, \ell k}) \in V^f$ we have

$$\begin{aligned}
\|w\|^2 &= \sum_{x \in \mathcal{N}} v(x) a(\phi_x - \phi_{x, \ell k}, \zeta_x w + b_x) \\
&\leq \sum_{x \in \mathcal{N}} |v(x)| \|\phi_x - \phi_{x, \ell k}\| \cdot (\|\zeta_x w\| + C'_{\mathfrak{S}_H} \|\mathfrak{S}_H((1 - \zeta_x)w)\|_{\omega_{x, \ell k+3}}) \\
&\leq 2C'_{\mathfrak{S}_H} C_{\mathfrak{S}_H} \sum_{x \in \mathcal{N}} |v(x)| \|\phi_x - \phi_{x, \ell k}\| \cdot (\|\zeta_x w\| + \|w\|_{\omega_{x, \ell k+4}}) \\
&\leq 2C'_{\mathfrak{S}_H} C_{\mathfrak{S}_H} \beta \sum_{x \in \mathcal{N}} |v(x)| \|\phi_x - \phi_{x, \ell k}\| \cdot \|(\nabla \zeta_x)(1 - \mathfrak{S}_H)w\|_{L^2(\omega_{x, \ell k+2})} \\
&\quad + 2C'_{\mathfrak{S}_H} C_{\mathfrak{S}_H} \sum_{x \in \mathcal{N}} |v(x)| \|\phi_x - \phi_{x, \ell k}\| \cdot \|w\|_{\omega_{x, \ell k+4}} \\
&\leq 2C'_{\mathfrak{S}_H} C_{\mathfrak{S}_H}^2 \frac{\beta}{\alpha} C_{\text{co}} \sum_{x \in \mathcal{N}} |v(x)| \|\phi_x - \phi_{x, \ell k}\| \cdot \|w\|_{\omega_{x, \ell k+4}} \\
&\leq 4C'_{\mathfrak{S}_H} C_{\mathfrak{S}_H}^2 \frac{\beta}{\alpha} C_{\text{co}} C_{\text{ov}}(\ell k)^{d/2} \left(\sum_{x \in \mathcal{N}} v^2(x) \|\phi_x - \phi_{x, \ell k}\|^2 \right)^{1/2} \|w\|,
\end{aligned}$$

where $C_{\text{ov}}(\ell k)^d$ is an upper bound on the number of patches $\omega_{x, \ell k}$ that overlap a single element in the mesh. The result follows by dividing by $\|w\|$ on both sides. \blacksquare

Theorem 8 Let $u \in V$ solve (2) and, given $\ell, k \geq 2 \in \mathbb{N}$, let $u_{H, \ell k}^{\text{ms}} \in V_{H, \ell k}^{\text{ms}}$ solve (12). Then

$$\|u - u_{H, \ell k}^{\text{ms}}\| \leq C_4 \alpha^{-1} \|H_T^{-1}\|_{L^\infty(\Omega)} (\ell k)^{d/2} (C_1/\ell)^{\frac{k-2}{2}} \|f\|_{L^2(\Omega)} + C_{\mathfrak{S}_H} \alpha^{-1} \|Hf\|_{L^2(\Omega)}.$$

holds with C_1 from Lemma 6 and a constant C_4 that depends on β/α , and ρ but not on H, k, ℓ, f , or u .

Proof. Let $\tilde{u}_{H, \ell k}^{\text{ms}} := \sum_{x \in \mathcal{N}} u_H^{\text{ms}}(x) (\lambda_x - \phi_{x, \ell k})$, where $u_H^{\text{ms}}(x)$, $x \in \mathcal{N}$, are the coefficients in the basis representation of u_H^{ms} . Due to Galerkin orthogonality, Lemma 3, Lemma 7, and the triangle inequality,

$$\begin{aligned}
\|u - u_{H, \ell k}^{\text{ms}}\|^2 &\leq \|u - \tilde{u}_{H, \ell k}^{\text{ms}}\|^2 = \|u - u_H^{\text{ms}} + u_H^{\text{ms}} - \tilde{u}_{H, \ell k}^{\text{ms}}\|^2 \\
&\leq C_{\mathfrak{S}_H}^2 \alpha^{-2} \|Hf\|_{L^2(\Omega)}^2 + C_3 (\ell k)^d \sum_{x \in \mathcal{N}} u_H^{\text{ms}}(x)^2 \|\phi_x - \phi_{x, \ell k}\|^2. \quad (26)
\end{aligned}$$

The application of Lemma 6 yields

$$\sum_{x \in \mathcal{N}} u_H^{\text{ms}}(x)^2 \left\| \phi_x - \phi_{x, \ell k} \right\|^2 \leq C_2^2 (C_1/\ell)^{k-2} \sum_{x \in \mathcal{N}} u_H^{\text{ms}}(x)^2 \left\| \phi_x \right\|_{\omega_{x, \ell}}^2.$$

Furthermore, we have

$$\begin{aligned} \sum_{x \in \mathcal{N}} u_H^{\text{ms}}(x)^2 \left\| \phi_x \right\|_{\omega_{x, \ell}}^2 &\leq C_{\text{inv}} \sum_{T \in \mathcal{T}} H_T^{-2} \sum_{x \in T \cap \mathcal{N}} u_H^{\text{ms}}(x)^2 \left\| \lambda_x \right\|_{L^2(T)}^2 \\ &\leq C'_{\text{inv}} \sum_{T \in \mathcal{T}} H_T^{-2} \left\| \sum_{T \cap \mathcal{N}} u_H^{\text{ms}}(x) \lambda_x \right\|_{L^2(T)}^2 \\ &= C'_{\text{inv}} \left\| H^{-2} \sum_{x \in \mathcal{N}} u_H^{\text{ms}}(x) \lambda_x \right\|_{L^2(\Omega)}^2 \\ &\leq C'_{\text{inv}} \|H^{-2} u_H^{\text{ms}}\|_{L^2(\Omega)}^2 + C'_{\text{inv}} \left\| H^{-2} \sum_{x \in \mathcal{N}} u_H^{\text{ms}}(x) (\phi_x - \mathfrak{S}_H \phi_x) \right\|_{L^2(\Omega)}^2 \\ &\leq C'_{\text{inv}} \alpha^{-1} (C_F \|H_T^{-2}\|_{L^\infty(\Omega)} + C_{\mathfrak{S}_H}) \left\| u_H^{\text{ms}} \right\|^2. \end{aligned}$$

where C'_{inv} and $C_{\mathfrak{S}_H}$ depend on ρ and C_F is the constant from Friedrichs' inequality. This yields

$$\begin{aligned} \left\| u_H^{\text{ms}} - u_{H, \ell k}^{\text{ms}} \right\| &\leq C_4 \|H_T^{-1}\|_{L^\infty(\Omega)} (\ell k)^{d/2} (C_1/\ell)^{(k-2)/2} \left\| u_H^{\text{ms}} \right\| \\ &\leq C_4 \|H_T^{-1}\|_{L^\infty(\Omega)} \alpha^{-1} (\ell k)^{d/2} (C_1/\ell)^{(k-2)/2} \|f\|_{L^2(\Omega)}, \end{aligned} \quad (27)$$

where C_4 only depends on $C_2, C_3, C'_{\text{inv}}, C_F,$ and $C_{\mathfrak{S}_H}$. The assertion follows readily by combining (26) and (27). ■

Remark 9 *The error estimate in Theorem 8 contains a factor $\|H^{-1}\|_{L^\infty(\Omega)}$. However, its influence on the total error can be controlled by choosing the localization parameter k proportional to $\log(1/\|H^{-1}\|_{L^\infty(\Omega)})$. For non-uniform meshes, it is recommended to vary the choice of the localization parameter in space according to $k \approx \log \frac{1}{H}$.*

4 Discretization of the Fine Scale Computations

In this section focus on how to compute numerical approximations to the local basis functions $\lambda_x - \phi_{x, \ell k}$ and there by to the multiscale solution $u_{H, \ell k}^{\text{ms}}$. In order to do this, we need to extend the error analysis of Section 3 to a fully discrete setting. There is a lot of freedom in choosing different finite elements and different refinement strategies, see e.g. [15, 16]. We will focus on a very simple and natural

approach, also considered in [17]. We assume that the local basis functions are computed using subgrids of a fine scale reference mesh, which is a (possibly space adaptive) refinement of the coarse grid \mathcal{T}_H .

More precisely, let \mathcal{T}_h be the result of one uniform refinement and several conforming but possibly non-uniform refinements of the coarse mesh \mathcal{T}_H . We introduce $h : \overline{\Omega} \rightarrow \mathbb{R}_{>0}$ as the \mathcal{T}_h -piecewise constant mesh width function with $h_t := h|_t = \text{diam}(t)$ for all $t \in \mathcal{T}_h$. We construct the finite element space

$$S_h := \{v \in C^0(\Omega) \mid \forall t \in \mathcal{T}_h(\Omega), v|_t \text{ is a polynomial of total degree } \leq 1\}.$$

We let $u_h \in V_h := S_h \cap H_0^1(\Omega)$ be the reference solution that satisfies

$$a(u_h, v) = F(v) \quad \text{for all } v \in V_h. \quad (28)$$

Locally on each patch we let

$$V_h^f(\omega_{x,k}) := V^f(\omega_{x,k}) \cap V_h = \{v \in V_h \mid \mathfrak{S}_H v = 0 \text{ and } v|_{\Omega \setminus \omega_{x,k}} = 0\}. \quad (29)$$

The numerical approximation $\phi_{x,k}^h \in V_h^f(\omega_{x,k})$ of the corrector $\phi_{x,k}^h$ is determined by

$$a(\phi_{x,k}^h, w) = a(\lambda_x, w) \quad \text{for all } w \in V_h^f(\omega_{x,k}).$$

We denote the discrete multiscale finite element space

$$V_{H,k}^{\text{ms},h} = \text{span}\{\lambda_x - \phi_{x,k}^h \mid x \in \mathcal{N}\}.$$

The corresponding discrete multiscale approximation $u_{H,k}^{\text{ms},h} \in V_{H,k}^{\text{ms},h}$ fulfills

$$a(u_{H,k}^{\text{ms},h}, v) = F(v) \quad \text{for all } v \in V_{H,k}^{\text{ms},h}. \quad (30)$$

Theorem 10 *Let $u \in V$ solve (2) and let $u_{H,\ell k}^{\text{ms},h} \in V_{H,k}^{\text{ms},h}$ solve (30). Then*

$$\| \|u - u_{H,\ell k}^{\text{ms},h}\| \| \leq \tilde{C}_4 \|H_T^{-1}\|_{L^\infty(\Omega)} (\ell k)^{d/2} (\tilde{C}_1/\ell)^{\frac{k-2}{2}} \|f\|_{L^2(\Omega)} + C_{\mathfrak{S}_H} \alpha^{-1} \|Hf\|_{L^2(\Omega)} + \|u - u_h\|.$$

Remark 11 (Multiscale splitting by nodal interpolation) *Having discretized the fine scale computation, i.e., having replaced the infinite dimensional space V by some finite element space $V_h \subset C^0(\overline{\Omega})$ we are allowed to replace the Clément-type interpolation by classical nodal interpolation. This leads to the variational multiscale method in [16]. Because nodal interpolation satisfies the conditions (6.a)–(6.b), Theorem 10 establishes an a priori error bound for the multiscale method [16].*

Remark 12 (Estimates for the fine scale error) *The finite element space V_h may be replaced by any finite element space that contains V_h , e.g., by piecewise polynomials of higher order. The third part in the error bound in Theorem 10 can be bounded in terms of data, mesh parameter h , and polynomial degree using standard a priori error estimates. For example, if $A \in W^{1,\infty}(\Omega)$ (bounded with bounded weak derivative) and ε is the smallest present scale, i.e., $\|\nabla A\|_{L^\infty(\Omega)} \lesssim \varepsilon^{-1}$, the third term in the error bound in Theorem 10 may be replaced by the worst case bound $Ch\varepsilon^{-1}$ for a first-order ansatz space V_h (see [20]). It is shown in [20] that for highly varying but smooth coefficient A , higher order ansatz spaces are superior.*

Remark 13 (Periodic coefficient) *Let Ω be some square or cube, $f \in L^2(\Omega)$, A be smooth and periodic, $A(x) = A(x/\varepsilon)$, with some small scale parameter $\varepsilon > 0$, and let u_ε denote the corresponding solution of (2). Choose uniform meshes \mathcal{T}_H and \mathcal{T}_h with $H > \varepsilon > h$ and $k \approx \log(H^{-1})$. With regard to the previous comment, Theorem 10 yields the error bound*

$$\| \| u_\varepsilon - u_{H,\ell k}^{\text{ms},h} \| \| \leq C_f (H + \frac{h}{\varepsilon}).$$

With $h \sim \varepsilon H$ the error in the approximation becomes independent of the fine scale oscillations without any so-called resonance effects as they are observed, e.g., in [12].

Remark 14 (Solution of the local problems) *The local problems need to be solved in the spaces $V_h^t(\omega_{x,k})$. This is a standard finite element space with the additional constraint that the trial and test functions should have no component in V_H . In practice this constraint is realized using Lagrange multipliers.*

The resulting coarse scale system of equations is of the same size as the original problem, $\dim(V_{H,k}^{\text{ms},h}) = \dim V_H$ and it is still sparse. The number of non-zero entries will be larger and depend on k . Note however that the non-zero entries in the stiffness matrix decay exponentially away from the diagonal.

Proof of Theorem 10. We use the triangle inequality $\| \| u - u_{H,\ell k}^{\text{ms},h} \| \| \leq \| \| u - u_h \| \| + \| \| u_h - u_H^{\text{ms},h} \| \| + \| \| u_H^{\text{ms},h} - u_{H,\ell k}^{\text{ms},h} \| \|$ and follow the arguments from the proof of Theorem 8 simply replacing V by V_h and using Lemmas 15, 17, and 18 below (discrete versions of Lemmas 3, 6, and 7) to bound the last two terms. ■

In the remaining part of this Section, $A \lesssim B$ abbreviates an inequality $A \leq C B$ with some generic constant $0 \leq C < \infty$ that does not depend on the mesh sizes H , h , and the localization parameters.

Lemma 15 (Discrete version of Lemma 3) *Let $u_h \in V_h$ solve (28) and $u_H^{\text{ms},h} \in V_H^{\text{ms},h}$ solve (30) with k large enough so that $\omega_{x,k} = \Omega$ for all $x \in \mathcal{N}$. Then*

$$\| \| u_h - u_H^{\text{ms},h} \| \| \leq C_{\text{ol}}^{1/2} C_{\mathfrak{S}_H} \alpha^{-1} \| Hf \|_{L^2(\Omega)}$$

holds with constants C_{ol} and $C_{\mathfrak{S}_H}$ that only depend on ρ .

Proof. Note that $u_h^f := u_h - u_H^{\text{ms},h}$ is the unique element of $V_h^f := V^f \cap V_h$ such that $a(u_h^f, v) = F(v)$ for all $v_f \in V_h^f$. The Lemma follows from the same arguments in the proof of Lemma 3. ■

To establish discrete versions of Lemmas 6 and 7 we are facing the technical difficulty that the product of $v \in V_h$ and some cut-off function η from Definition 5 is not necessarily an element of V_h . However, the subsequent lemma shows that the product ηv can be approximated sufficiently well by elements from V_h .

Lemma 16 *For all $x \in \mathcal{N}$, $D > d \in \mathbb{N}$, and corresponding cut-off function $\eta_x^{d,D}$ defined in (15) there exists some $v \in V_h^f(\omega_{x,D+1})$ such that*

$$\| \| \eta_x^{d,D} \phi_x^h - v \| \| \lesssim \frac{1}{D-d} \| h/H \|_{L^\infty(\omega_{x,D} \setminus \omega_{x,d})} \| \| \phi_x^h \| \|_{\omega_{x,D+1} \setminus \omega_{x,d-1}}.$$

Furthermore the statement also holds if $\eta_x^{d,D}$ is replaced by $1 - \eta_x^{d,D}$ and $v \in V_h^f(\Omega \setminus \omega_{x,d-1})$.

Proof. Let $x \in \mathcal{N}$, $D > d \in \mathbb{N}$ be fixed and define $\eta := \eta_x^{d,D}$. Let $\mathfrak{S}_h : V \cap C(\bar{\Omega}) \rightarrow V^h$ be the nodal interpolant with respect to the mesh \mathcal{T}_h . Recall its (local) approximation and stability properties

$$\| \nabla(v - \mathfrak{S}_h v) \|_{L^2(t)} \lesssim h_t \| \nabla^2 v \|_{L^2(t)} \quad \text{and} \quad \| \mathfrak{S}_h v \|_{L^2(t)} \lesssim \| v \|_{L^2(t)}$$

for all polynomials v . According to Lemma 1, there exists some $b_x \in V^h$ such that $\mathfrak{S}_H(b_x) = \mathfrak{S}_H(\mathfrak{S}_h(\eta \phi_x^h))$, $\| \| b_x \| \| \lesssim \| \| \mathfrak{S}_H(\mathfrak{S}_h(\eta \phi_x^h)) \| \|$, and $\text{supp}(b_x) \subset \omega_{x,D+1} \setminus \omega_{x,d-1}$. Hence, $v := \mathfrak{S}_h(\eta \phi_x^h) - b_x \in V_h^f(\omega_{x,D+1})$. Since $\mathfrak{S}_H \bar{\eta}_t \phi_x^h = 0$ for $\bar{\eta}_t = |t|^{-1} \int_t \eta(y) dy$, we get

$$\begin{aligned} \| \| \eta \phi_x^h - v \| \|^2 &= \| \| \eta \phi_x^h - \mathfrak{S}_h(\eta \phi_x^h) + b_x \| \|^2 \\ &\lesssim \sum_{t \in \mathcal{T}_h: t \subset \bar{\omega}_{x,D} \setminus \omega_{x,d}} \| \nabla(\eta \phi_x^h - \mathfrak{S}_h(\eta \phi_x^h)) \|_{L^2(t)}^2 + \| \| \mathfrak{S}_H(\mathfrak{S}_h(\eta \phi_x^h)) \| \|^2 \\ &\lesssim \sum_{t \in \mathcal{T}_h: t \subset \bar{\omega}_{x,D} \setminus \omega_{x,d}} h_t^2 \| \nabla^2(\eta \phi_x^h) \|_{L^2(t)}^2 + \sum_{T \in \mathcal{T}_H: T \subset \bar{\omega}_{x,D+1} \setminus \omega_{x,d-1}} H_T^{-2} \sum_{t \in \mathcal{T}_h: t \subset T} \| \mathfrak{S}_h((\eta - \bar{\eta}_t) \phi_x^h) \|_{L^2(t)}^2 \\ &\lesssim \sum_{t \in \mathcal{T}_h: t \subset \bar{\omega}_{x,D} \setminus \omega_{x,d}} h_t^2 \| \nabla^2(\eta \phi_x^h) \|_{L^2(T)}^2 + \sum_{T \in \mathcal{T}_H: T \subset \bar{\omega}_{x,D+1} \setminus \omega_{x,d-1}} H_T^{-2} \sum_{t \in \mathcal{T}_h: t \subset T} \| (\eta - \bar{\eta}_t) \|_{L^\infty(t)}^2 \| \phi_x^h \|_{L^2(t)}^2 \\ &\lesssim \sum_{T \in \mathcal{T}_H: T \subset \bar{\omega}_{x,D+1} \setminus \omega_{x,d-1}} \| h \|_{L^\infty(T)}^2 \| \nabla \eta \|_{L^\infty(T)}^2 \| \| \phi_x^h \| \|^2_T. \end{aligned}$$

The first part of the Lemma now follows using the property (14.c) of η . The second part concerning $1 - \eta$ follows using the same argument but with $v \in V_h^f(\Omega \setminus \omega_{x,d-1})$.

■

Lemma 17 (Discrete version of Lemma 6) *For all $x \in \mathcal{N}$, $k, \ell \geq 2 \in \mathbb{N}$ the estimate*

$$\|\|\phi_x^h - \phi_{x,\ell k}^h\|\| \leq \tilde{C}_2 \left(\frac{\tilde{C}_1}{\ell}\right)^{\frac{k-2}{2}} \|\|\phi_x^h\|\|_{\omega_{x,\ell}}$$

holds with constants \tilde{C}_1, \tilde{C}_2 that only depend on ρ but not on x, k, ℓ, h , or H .

Proof. Let $\zeta_x := 1 - \eta_x^{\ell(k-1)+1, \ell k-1}$ with $\eta_x^{\ell(k-1)+1, \ell k-1}$ as in equation (15) in Definition 5. Then there exists a $v \in V_h^f(\omega_{x,\ell k})$ such that,

$$\begin{aligned} \|\|\phi_x^h - v\|\|_{\omega_{x,\ell k}} &\leq \|\|\phi_x^h - \zeta_x \phi_x^h\|\|_{\omega_{x,\ell k}} + \|\|\zeta_x \phi_x^h - v\|\|_{\omega_{x,\ell k}} \\ &\lesssim \|\|\phi_x^h\|\|_{\omega_{x,\ell k} \setminus \omega_{x,\ell(k-1)+1}} + \|\|\zeta_x \phi_x^h\|\|_{\omega_{x,\ell k-1} \setminus \omega_{x,\ell(k-1)+1}}. \end{aligned}$$

Furthermore, using the same argument as in Lemma 6,

$$\|\|\zeta_x \phi_x^h\|\|_{\omega_{x,\ell k-1} \setminus \omega_{x,\ell(k-1)+1}} \lesssim \|\|\phi_x^h\|\|_{\omega_{x,\ell k} \setminus \omega_{x,\ell(k-1)+1}}$$

which yields

$$\|\|\phi_x^h - \phi_{x,\ell k}^h\|\| \leq \|\|\phi_x^h - v\|\|_{\omega_{x,\ell k}}^2 + \|\|\phi_x^h\|\|_{\Omega \setminus \omega_{x,\ell k}} \lesssim \|\|\phi_x^h\|\|_{\Omega \setminus \omega_{x,\ell(k-1)+1}}.$$

Now let $\eta_j := \eta_x^{\ell(j-1)+1, \ell j}$ (cf. Definition 5), $j = 2, 3, \dots, k-1$ and note that

$$\|A^{1/2} \nabla \phi_x^h\|_{L^2(\Omega \setminus \omega_{x,\ell(k-1)})}^2 \leq a(\phi_x^h, \eta_{k-1}^2 \phi_x^h) - 2 \int_{\Omega} \eta_{k-1} \phi_x^h \langle A \nabla \phi_x^h, \nabla \eta_{k-1} \rangle dx.$$

The second term can be treated exactly as in Lemma 6 and, hence, bounded by $\ell^{-2} \|\|\phi_x^h\|\|_{\Omega \setminus \omega_{x,\ell(k-2)}}^2$. We make use of Lemma 16 to bound the first term. There exists $v \in V_h^f(\Omega \setminus \omega_{x,\ell(k-1)+1})$ such that

$$a(\phi_x^h, \eta_{k-1}^2 \phi_x^h) \leq \|\|\phi_x^h\|\|_{\omega_{\ell(k-1)} \setminus \omega_{\ell(k-2)+1}} \|\|\eta_{k-1}^2 \phi_x^h - v\|\| \lesssim \ell^{-2} \|\|\phi_x^h\|\|_{\Omega \setminus \omega_{x,\ell(k-2)}}^2.$$

The final assertion follows by similar arguments as in the proof of Lemma 6. ■

Lemma 18 (Discrete version of Lemma 7) *There is a constant \tilde{C}_3 depending only on ρ and β/α , but not on $|\mathcal{N}|, k$, or ℓ such that,*

$$\left\| \sum_{x \in \mathcal{N}} v(x) (\phi_x^h - \phi_{x,\ell k}^h) \right\|^2 \leq \tilde{C}_3 (\ell k)^d \sum_{x \in \mathcal{N}} v^2(x) \|\|\phi_x^h - \phi_{x,\ell k}^h\|\|^2.$$

Proof. For $x \in \mathcal{N}$, let $\zeta_x = 1 - \eta_x^{\ell k+1, \ell k+2}$ (cf. Definition 5) and $z = \sum_{x \in \mathcal{N}} v(x) (\phi_x - \phi_{x, \ell k})$. We have,

$$\left\| \sum_{x \in \mathcal{N}} v(x) (\phi_x - \phi_{x, \ell k}) \right\|^2 = \sum_{x \in \mathcal{N}} v(x) a(\phi_x^h - \phi_{x, \ell k}^h, \zeta_x z + (1 - \zeta_x)z) = \text{I} + \text{II}.$$

The first term $\text{I} := \sum_{x \in \mathcal{N}} v(x) a(\phi_x^h - \phi_{x, \ell k}^h, \zeta_x z)$ can be treated in exactly the same way as in the proof of Lemma 7. We focus on the second term. Due to Lemma 16 there exists a $w \in V_h^f(\Omega \setminus \omega_{\ell k})$ such that

$$\begin{aligned} \text{II} &:= \sum_{x \in \mathcal{N}} v(x) a(\phi_x^h - \phi_{x, \ell k}^h, (1 - \zeta_x)z - w) \\ &\lesssim \left(\sum_{x \in \mathcal{N}} |v(x)|^2 \left\| \phi_x^h - \phi_{x, \ell k}^h \right\|^2 \right)^{1/2} \left(\sum_{x \in \mathcal{N}} \left\| (1 - \zeta_x)z - w \right\|^2 \right)^{1/2} \\ &\lesssim \left(\sum_{x \in \mathcal{N}} |v(x)|^2 \left\| \phi_x^h - \phi_{x, \ell k}^h \right\|^2 \right)^{1/2} \left(\sum_{x \in \mathcal{N}} \left\| z \right\|_{\omega_{x, \ell k+2} \setminus \omega_{\ell k+1}}^2 \right)^{1/2} \\ &\lesssim (\ell k)^{d/2} \left(\sum_{x \in \mathcal{N}} |v(x)|^2 \left\| \phi_x^h - \phi_{x, \ell k}^h \right\|^2 \right)^{1/2} \left\| z \right\|. \end{aligned}$$

The result follows immediately. ■

5 Numerical Experiments

Numerical experiments shall validate our theoretical results from the previous sections.

5.1 Experimental setup

Let Ω be the unit square and the outer force $f \equiv 1$ in Ω . Consider three different choices for the scalar coefficient A_1, A_2, A_3 with increasing difficulty as depicted in Figure 1. The coefficient $A_1 = 1$ is constant. The coefficient A_2 is piecewise constant with respect to a uniform Cartesian grid of width 2^{-6} . The values in each grid cell are chosen in the range $[1/20, 2]$; the contrast $\beta(A_2)/\alpha(A_2) \leq 40$ is moderate. The coefficient A_3 is piecewise constant with respect to the same uniform Cartesian grid of width 2^{-6} . Its values are taken from the data of the SPE10 benchmark, see <http://www.spe.org/web/csp/>. The contrast for A_3 is large, $\beta(A_3)/\alpha(A_3) \approx 4 \cdot 10^6$. Consider uniform coarse meshes of size $H = 2^{-1}, 2^{-2}, \dots, 2^{-6}$ of Ω as depicted in Figure 2. Note that none of these meshes resolves the rough coefficients A_2 and A_3 appropriately.

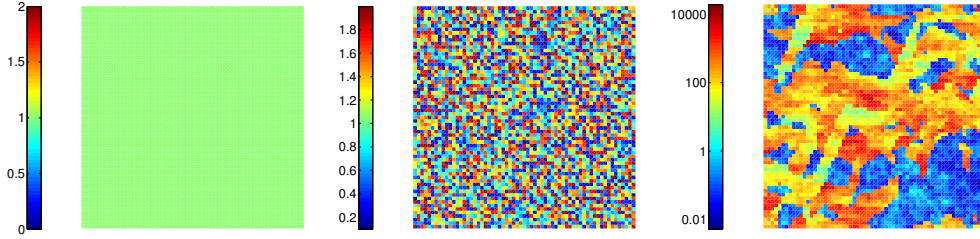


Figure 1: Scalar coefficient used in the numerical experiment: A_1 (left), A_2 (middle), A_3 (right).

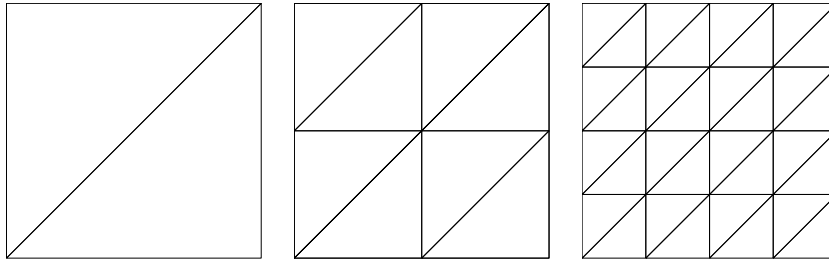


Figure 2: Uniform triangulations of the unit square.

The reference mesh \mathcal{T}_h has width $h = 2^{-9}$. Since no analytical solutions are available, the standard finite element approximation $u_h \in V_h$ on the reference mesh \mathcal{T}_h serves as the reference solution. The approximations are compared with this reference solution only. Doing this, we assume that u_h is sufficiently accurate. All fine scale computations are performed on subsets of \mathcal{T}_h .

5.2 Results for the energy error

Figure 3 depicts the energy errors of the new multiscale method and the classical P1FEM (see (3)) with respect to the same coarse mesh. Depending on the coarse discretization scale H , the localization parameter k is chosen to be $\lceil 2 \log(1/H) \rceil$. The logarithmic dependence on $1/H$ is motivated by our a priori analysis. The choice of the constant 2 is based on numerical tests. It turns out that, in all experiments, this choice leads to the desired linear textbook convergence (rate $-1/2$) of the energy error (w.r.t. to the number of degrees of freedom $N_{\text{dof}} = |\mathcal{N}| \approx H^{-2}$) related to the sequence of multiscale approximations. Pre-asymptotic effects are not observed. In particular, the performance of our method does not seem to be affected by the high contrast present in A_3 . Whether our estimates on the decay of the corrector functions are sub-optimal or have worst-case character with respect

to contrast is an issue of present research.

Observe that the classical P1FEM suffers from the lacks of approximability and regularity and converges only poorly for the rough coefficients A_2 and A_3 .

5.3 Results for the L^2 error

Figure 4 shows L^2 errors of the new multiscale method and the classical P1FEM. Again, the choice of the localization parameter $k = \lceil 2 \log(1/H) \rceil$ yields the optimal convergence rate -1 for our method in all experiments (w.r.t. to the number of degrees of freedom $N_{dof} = |\mathcal{N}| \approx H^{-2}$) without any pre-asymptotic behavior.

More importantly, we observe that the L^2 error between u_h and $\mathfrak{S}_H u_{H,k}^{ms,h}$ converges nicely at a rate close to $-3/4$. This is remarkable because, $\mathfrak{S}_H u_{H,k}^{ms,h}$ is a true coarse approximation. $\mathfrak{S}_H u_{H,k}^{ms,h}$ is an element of the coarse $P1$ finite element space. Hence, it cannot capture microscopic features of the solution. The rate of convergence is limited by $\frac{1+s}{2}$ for some $s \in [0, 1]$ which is related to the regularity of the solution ($u \in H^{1+s}$ for some $s \in [0, 1]$). However, in contrast to the classical P1FEM approximation u_H , $\mathfrak{S}_H u_{H,k}^{ms,h}$ converges at some rate better than $-1/2$ and, hence, allows to approximate the macroscopic behavior of the solution very accurately with only very few degrees of freedom. Note that the storage complexity of the modified basis is of order $\mathcal{O}(h^{-2} \log 1/H)$ whereas its interpolation can be stored in $\mathcal{O}(H^{-2} \log 1/H)$. Once the system matrix of the multiscale method is assembled, $\mathfrak{S}_H u_{H,k}^{ms,h}$ can be computed without using the modified basis whereas this would be required to represent $u_{H,k}^{ms,h}$.

6 Application to Multiscale Methods

In this section we discuss three multiscale methods and how the presented analysis relates to each of them.

6.1 The Variational Multiscale Method

The variational multiscale method was first introduced in [13]. The function space V is here split into a coarse part (standard finite element space on a coarse mesh), in our case V_H , and a fine part, in our case V^f . The weak form is then also decoupled into a coarse and a fine part. The method reads: find $\bar{u} \in V_H$ and $u' \in V^f$ such that,

$$\begin{aligned} a(\bar{u}, \bar{v}) + a(u', \bar{v}) &= F(\bar{v}) \quad \text{for all } \bar{v} \in V_H, \\ a(u', v') &= F(v') - a(\bar{u}, v') \quad \text{for all } v' \in V^f. \end{aligned}$$

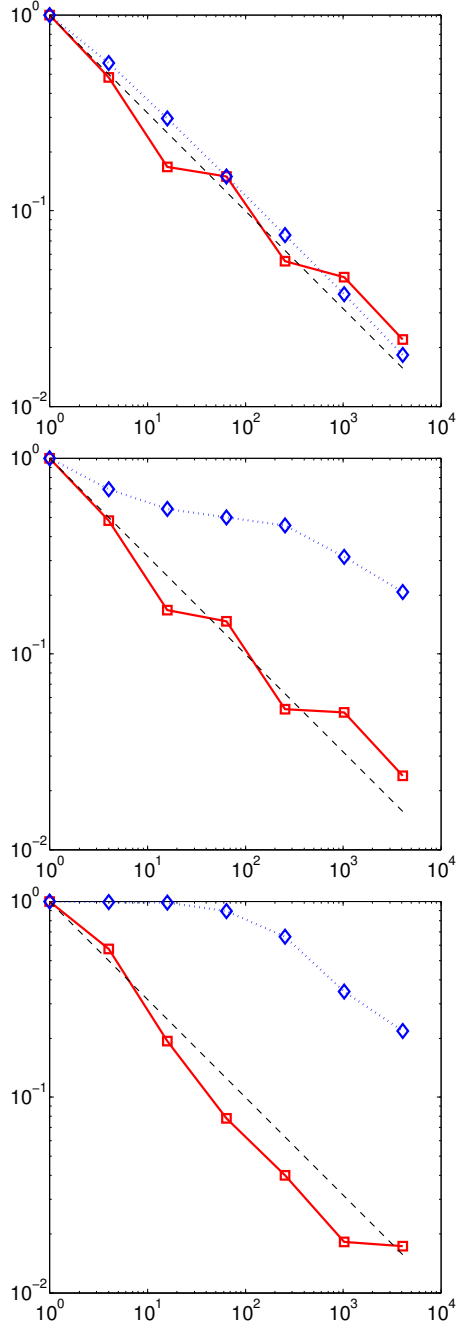


Figure 3: Relative energy errors $\|u_h - u_{H,k}^{\text{ms},h}\| / \|u_h\|$ (\square solid red) with localization parameter $k = \lceil 2 \log(1/H) \rceil$ and $\|u_h - u_H\| / \|u_h\|$ (\diamond dotted blue) vs. number of degrees of freedom $N_{\text{dof}} \approx H^{-2}$ for different coefficients: A_1 (top), A_2 (middle), A_3 (bottom). The dashed black line is $N_{\text{dof}}^{-1/2}$.

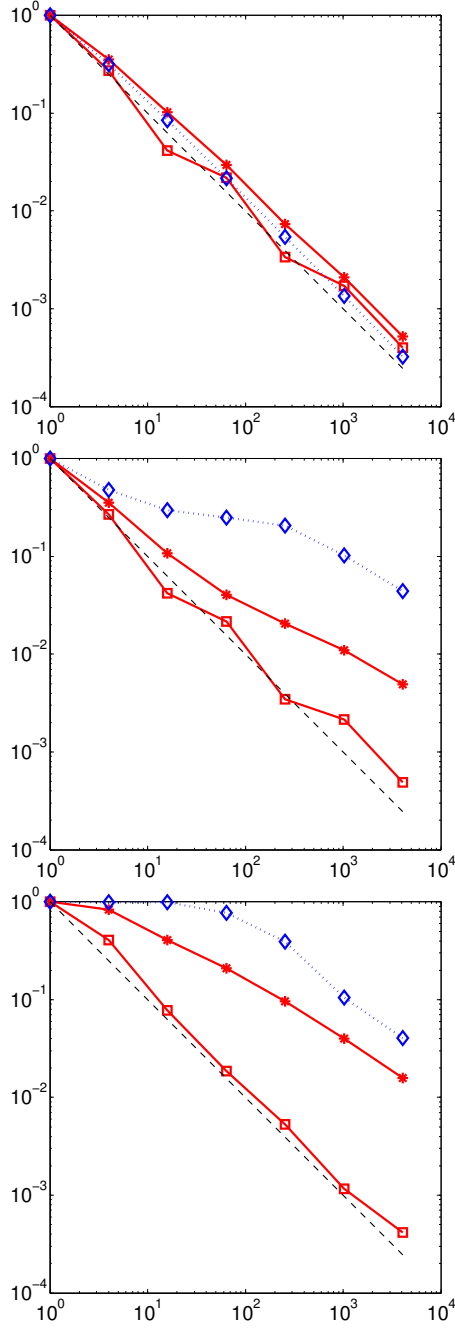


Figure 4: Relative L^2 errors $\|u_h - u_{H,k}^{\text{ms},h}\|/\|u_h\|$ (\square solid red), $\|u_h - \mathfrak{I}_H u_{H,k}^{\text{ms},h}\|/\|u_h\|$ ($*$ solid red) with localization parameter $k = \lceil 2 \log(1/H) \rceil$ and $\|u_h - u_H\|/\|u_h\|$ (\diamond dotted blue) vs. number of degrees of freedom $N_{\text{dof}} \approx H^{-2}$ for different coefficients: A_1 (top), A_2 (middle), A_3 (bottom). The dashed black line is N_{dof}^{-1} .

The fine scale solution is further decoupled over the coarse elements $T \in \mathcal{T}_H$ and approximated using analytical techniques. Note that the fine scale solution u' is an affine map of the coarse scale solution \bar{u} . If we let $u' \approx M\bar{u} + m$ and plug this in to the method we get a coarse stiffness matrix of the form $a(\bar{v} + M\bar{v}, \bar{w})$, i.e., a non-symmetric bilinear form for a symmetric problem.

6.2 The Multiscale Finite Element Method

In [12] the multiscale finite element method was first introduced. Here modified multiscale basis functions are computed numerically on sub-grids on each coarse element individually. The basis functions fulfill: find $\phi_{x,T} \in H_0^1(T)$

$$a(\lambda_x - \phi_{x,T}, v) = 0 \quad \text{for all } v \in H_0^1(T) \text{ and for all } T \in \mathcal{T}_H.$$

Here homogeneous Dirichlet boundary conditions are used on the boundary of each element T , i.e., the local problems are totally decoupled. To get a more accurate method one can improve the boundary conditions using information from the data A . A larger domain can also be considered (this procedure is referred to as over-sampling), see e.g. [12]. Note that since the coarse scale basis functions are modified (both trial and test space) the resulting method is symmetric.

6.3 The Proposed Method

The modified basis function construction given by equation (8-9) was first introduced in a variational multiscale framework in [14, 15]. In these papers the Scott-Zhang interpolation was used in the analysis and nodal interpolation in the discrete setting for the numerical examples. The method has also been used to modify basis functions in the spirit of the multiscale finite element method, see e.g. [18]. The exponential decay in terms of layers of coarse elements have been demonstrated numerically in several works, see e.g. [16, 18, 17]. In all experiments considered in these papers, the fixed choice of two or three layers of coarse elements in the patches appeared sufficiently accurate for engineering purposes. The first paper where the exponential decay was analyzed is [17]. The theory of iterative solvers was used to show convergence to a discrete reference solution.

The proposed method has been extended to convection dominated problems and problems in mixed form [18] as well as time dependent problems [19]. A posteriori error bounds have been derived and adaptive algorithms designed where the local mesh and patch size are chosen automatically in order to reduce the error.

6.4 Application of the Presented Analysis

The convergence proof in this paper generalizes the results of [17] and gives a valid bound also as $h \rightarrow 0$ independent of the patch size and coarse mesh size. The proof does not rely on regularity of the solution and gives a very explicit expression for the rate of convergence. The present analysis confirms the numerical results in [16, 18, 17] and gives together with [17] the method the solid theoretical foundation that has previously been missing. The analysis also justifies the use of a posteriori error bounds for adaptivity [15, 18] because we can now prove that the quantities measured on the patch boundary decays exponentially in the number of coarse layers.

For the variational multiscale method this result says that it is important to allow larger subgrid patches than just one coarse element. This will result in overlap but the local problems are totally decoupled and we have in previous works demonstrated how adaptivity can be used to only solve local problems where it is needed, see for instance [15, 18]. For the multiscale finite element method the analysis is not directly applicable since the fine scale space V^f is not used. It is the decay in this space which we have proven to be exponential (in number of coarse layers of elements in the subgrid). If this decay is not present, inhomogeneous boundary conditions are instead needed for the subgrid problems. To the best of our knowledge, such constructions have only been proved to be accurate in special settings, e.g., periodic coefficients.

References

- [1] I. Babuška, G. Caloz, and J. E. Osborn. Special finite element methods for a class of second order elliptic problems with rough coefficients. *SIAM J. Numer. Anal.*, 31(4):945–981, 1994.
- [2] I. Babuška and R. Lipton. The penetration function and its application to microscale problems. *Multiscale Model. Simul.*, 9(1):373–406, 2011.
- [3] I. Babuška and J. E. Osborn. Generalized finite element methods: their performance and their relation to mixed methods. *SIAM J. Numer. Anal.*, 20(3):510–536, 1983.
- [4] I. Babuška and J. E. Osborn. Can a finite element method perform arbitrarily badly? *Math. Comp.*, 69(230):443–462, 2000.
- [5] I. Babuška and J. M. Melenk. The partition of unity method. *International Journal of Numerical Methods in Engineering*, 40:727–758, 1996.

- [6] L. Berlyand and H. Owhadi. Flux norm approach to finite dimensional homogenization approximations with non-separated scales and high contrast. *Arch. Ration. Mech. Anal.*, 198(2):677–721, 2010.
- [7] F. Brezzi, L. Franca, T. Hughes, and A. Russo. $b = \int g$. *Comput. Methods Appl. Mech. Engrg.*, 145:329–339, 1997.
- [8] C. Carstensen and R. Verfürth. Edge residuals dominate a posteriori error estimates for low order finite element methods. *SIAM J. Numer. Anal.*, 36(5):1571–1587 (electronic), 1999.
- [9] P. Ciarlet. *The finite element method for elliptic problems*. North-Holland, 1987.
- [10] P. Clément. Approximation by finite element functions using local regularization. *Rev. Française Automat. Informat. Recherche Opérationnelle Sér. RAIRO Analyse Numérique*, 9(R-2):77–84, 1975.
- [11] L. Grasedyck, I. Greff, and S. Sauter. The AL Basis for the Solution of Elliptic Problems in Heterogeneous Media. Technical report, Institut für Mathematik, Universität Zürich, Preprint 02-2011, 2011.
- [12] T. Y. Hou and X.-H. Wu. A multiscale finite element method for elliptic problems in composite materials and porous media. *J. Comput. Phys.*, 134(1):169–189, 1997.
- [13] T. J. R. Hughes, G. R. Feijóo, L. Mazzei, and J.-B. Quinicy. The variational multiscale method—a paradigm for computational mechanics. *Comput. Methods Appl. Mech. Engrg.*, 166(1-2):3–24, 1998.
- [14] M. G. Larson and A. Målqvist. Adaptive variational multiscale methods based on a posteriori error estimation: duality techniques for elliptic problems. In *Multiscale methods in science and engineering*, volume 44 of *Lect. Notes Comput. Sci. Eng.*, pages 181–193. Springer, Berlin, 2005.
- [15] M. G. Larson and A. Målqvist. Adaptive variational multiscale methods based on a posteriori error estimation: energy norm estimates for elliptic problems. *Comput. Methods Appl. Mech. Engrg.*, 196(21-24):2313–2324, 2007.
- [16] M. G. Larson and A. Målqvist. A mixed adaptive variational multiscale method with applications in oil reservoir simulation. *Math. Models Methods Appl. Sci.*, 19(7):1017–1042, 2009.

- [17] A. Målqvist. A priori error analysis of a multiscale method. *Preprint*.
- [18] A. Målqvist. Multiscale methods for elliptic problems. *Multiscale Model. Simul.*, 9:1064–1086, 2011.
- [19] J. M. Nordbotten. Adaptive variational multiscale methods for multiphase flow in porous media. *Multiscale Model. Simul.*, 7(3):1455–1473, 2008.
- [20] D. Peterseim and S. A. Sauter. Error estimates for finite element discretizations of elliptic problems with oscillatory coefficients. *DFG Research Center Matheon Berlin, Preprint Series, 756*, 2011.
- [21] H. Owhadi and L. Zhang. Localized bases for finite-dimensional homogenization approximations with nonseparated scales and high contrast. *Multiscale Modeling & Simulation*, 9(4):1373–1398, 2011.